Design Criteria and Error Sensitivity of Time-Domain Channel Characterization (TCC) for Asymmetry Fixture De-Embedding

Changwook Yoon, *Member, IEEE*, Mikheil Tsiklauri, *Member, IEEE*, Mikhail Zvonkin, Qinghua Bill Chen, Alexander Razmadze, Aman Aflaki, Jingook Kim, *Member, IEEE*, Jun Fan, *Senior Member, IEEE*, and James L. Drewniak, *Fellow, IEEE*

***Abstract*—Time-domain channel characterization (TCC) for de-embedding of an asymmetric fixture is introduced. Two design criteria for the design of a 2x-thru are proposed. Error sensitivity regarding a small error in the S-parameters of the 1x-fixture is analyzed with an insertion loss error-coefficient and a return loss error-coefficient. The TCC procedure, including proposed design criteria and error sensitivity, is also introduced to reduce the error in the TCC application. Three different 2x-thru structures are investigated for the verification of the two proposed design criteria and analyzed for error sensitivity. Test fixtures on a printed circuit boards are fabricated for the experimental verification.**

***Index Terms*—De-embedding, design criteria, error-coefficient, error sensitivity, insertion loss error-coefficient (ILEC), return loss error-coefficient (RLEC), time-domain channel characterization (TCC).**

I. Introduction

As data rates on both single-ended and differential channels on printed circuit boards (PCBs) increase and timing error budgets become tight, de-embedding of undesired fixtures along with a channel has become more important and increasingly critical. Most high-speed I/O channels, consisting of many undesired fixtures, such as ball-pads, vias, and connectors, are inevitably included in the measured timing error. These undesired fixtures make the timing error bigger, and this small error eventually brings a system failure in the test of high-speed signals. Thus, an accurate channel model and applying it into the de-embedding procedure after the measurement is required as a signal speed on that channel goes higher.

Manuscript received November 4, 2014; accepted December 1, 2014. Date of current version August 13, 2015. This work was supported in part by the National Science Foundation under Grant IIP-1440110.

C. Yoon and A. Aflaki are with the Altera Corporation, San Jose, CA 94089 USA (e-mail: Changwook.yoon@gmail.com; aaflaki@altera.com).

M. Tsiklauri, M. Zvonkin, J. Fan, and J. Drewniak are with the Department of Electrical Engineering, Missouri University of Science and Technology, Rolla, MO 65401 USA (e-mail: tsiklaurim@mst.edu; mzvx8@mst.edu; jfan@mst.edu; drewniak@mst.edu).

A. Razmadze is with the Apple, Cupertino, CA 95014 USA (e-mail: alexander.razmadze@gmail.com).

J. G. Kim is with the Electrical Engineering Department, Ulsan National Institute of Science and Technology, Ulju-gun, Ulsan 689-800, Korea (e-mail: jingook@unist.ac.kr).

Q. B. Chen is with the Yangtze Delta Region Institute of Tsinghua University, Tiaxing 100084, China, and also with the School of Software and Microelectronics, Peking University, Beijing 100080, China (e-mail: billchen@sanlogic.com).

Color versions of one or more of the figures in this paper are available online at http://ieeexplore.ieee.org.

Digital Object Identifier 10.1109/TEMC.2014.2379627

An equivalent lumped model based on a physical shape and material using a 2-D/3-D tool is the most popular and the fastest way to build the channel model [1], [2], [3]. This simple circuit model, consisting of a resistor, capacitor, and inductor, can be used for the simulation in time domain to predict the system budget and is applicable for de-embedding as a postprocess in frequency domain. However, the equivalent circuit model has a high accuracy only for simple shapes such as a rectangular transmission line surrounding homogeneous materials. Moreover, there is a bandwidth limitation to use. The accurate equivalent circuit model for more complicated shapes such as a ball or connector, is not easy to be modeled. Even though it is modeled, the small error in the modeling procedure eventually generates a big error after de-embedding that model.

Another popular de-embedding method is the well-known calibration SOLT and TRL [4], [5]. The calibration procedure is easily applicable for the complicated channel including non-ideal shapes which are not modeled in equivalent circuit modeling. Also, since analytical theory is very clear to understand, its useful bandwidth can be predetermined with the DUTs for the calibration. However, this calibration method has very high accuracy, only if the fixture is symmetrical and well-designed calibration DUTs are provided. If not, another procedure to remove error values at each port is necessary, and this additional postprocess easily generates a big error caused by unknown parasitic values. These parasitic values are not considerable at low frequency, but will be critical variables to amplify the error during de-embedding in the frequency domain.

A time-domain channel characterization (TCC) is one of the alternative methods for the asymmetric channel with the reflected waveform in the time domain [6], [7], [8]. The TCC method is only available on reciprocal and passive networks, and needs symmetry fixtures consisting of two channels to be deembedded. Since most symmetry fixtures are reciprocal and passive, the TCC method can be widely useful. However, the most difficult step in the TCC method is not the application, but the validation after the channel is estimated based on the TCC method. There is no way to know how accurate the calculated channel is, and how much the error will be amplified from the small error in the TCC method. Most research regarding the TCC method only focus on its final characterization result, compared with simulation data.

This paper proposes design criteria of the symmetry pattern to avoid the error value. Also, this paper analyzes the error

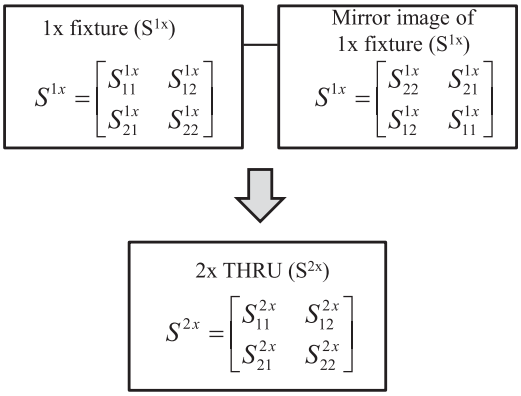

Fig. 1. Calibration pattern S-parameters consisting of a 1x-fixture cascaded with its mirror image to comprise the 2x-thru that is symmetric and $S_{11}^{2x} = S_{22}^{2x}, S_{21}^{2x} = S_{12}^{2x}$.

sensitivity to estimate the error amplification after de-embedding in the TCC procedure. Three test patterns on PCB were investigated to validate the proposed design criteria, and measured to verify the error sensitivity.

II. Time-Domain Channel Characterization

The TCC algorithm is detailed below, using frequency-domain S-parameter measurements in a symmetric calibration pattern and a DUT.

A. Symmetric Calibration Pattern—2x-Thru

In order to apply the TCC algorithm, a 2x-thru structure consisting of a 1x-fixture pattern and its mirror image is used. If the 1x-fixture is passive and reciprocal, then $\mathrm{S}_{21}^{1x} = \mathrm{S}_{12}^{1x}$, but the reflection looking in at opposite ends of the 1x-fixture are different so that $\mathrm{S}_{11}^{1x} \neq \mathrm{S}_{22}^{1x}$. The S-parameter blocks are shown schematically in Fig. 1 for the construction of the calibration pattern. After cascading the 1x-fixture and its mirror image, the resulting 2x-thru structure is symmetric, and $\mathrm{S}_{11}^{2x} = \mathrm{S}_{22}^{2x}, \mathrm{S}_{21}^{2x} = \mathrm{S}_{12}^{2x}$.

If all S-parameters in the TCC algorithm satisfy reciprocal and passive, and insertion loss (IL) and return loss (RL) in the S-parameters of the 2x-thru have a relationship with S-parameters of 1x-fixture, as expressed in

$$\mathrm{S}_{11}^{2x} = \mathrm{S}_{11}^{1x} + \frac{\left(\mathrm{S}_{21}^{1x}\right)^2 \mathrm{S}_{22}^{1x}}{1 - \left(\mathrm{S}_{22}^{1x}\right)^2} \tag{1}$$

$$\mathrm{S}_{21}^{2x} = \frac{\left(\mathrm{S}_{21}^{1x}\right)^2}{1 - \left(\mathrm{S}_{22}^{1x}\right)^2}. \tag{2}$$

Since TCC assumes that the S-parameters of the 2x-thru are known from the measurement, one more formula is necessary to calculate the S-parameters of the 1x-fixture. This is a simple algebraic formula about two equations and three unknown variable $[\mathrm{S}_{11}^{1x}, \mathrm{S}_{12}^{1x} = \mathrm{S}_{21}^{1x}, \mathrm{S}_{22}^{1x}]$.

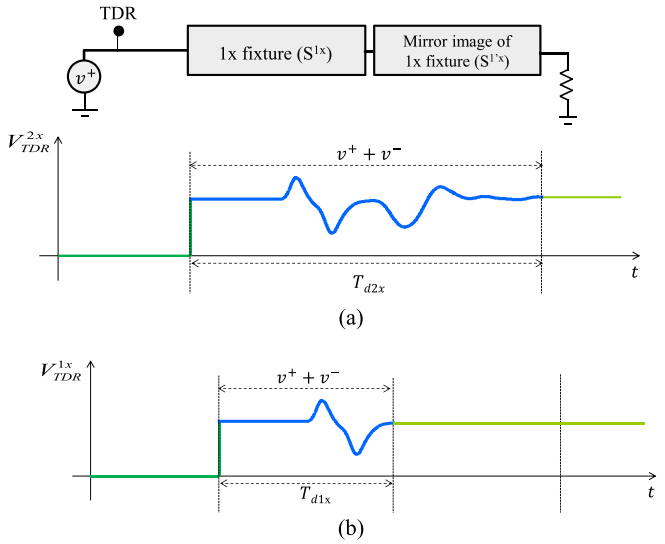

Fig. 2. TDR waveform in time domain from a 2x-thru (a) and modified TDR waveform to estimate the reflection ratio $[\Gamma_M^{1x}]$ from a 1x-fixture (b).

B. 1x-Fixture With TDR Waveform

In order to solve two equations with three unknown variables, TDR waveform is used as an additional way to provide one more equation. TDR waveform generally consists of an injection waveform $[v + (t)]$ and a reflection waveform $[v - (t)]$ in time domain, as expressed in (3), and shows discontinuity, then provides both mismatched levels along with the whole channel, as shown in Fig. 2(a). The measured reflection ratio Γ_M^{2x} can be defined as the ratio of incident voltage $[v + (f)]$ and reflected voltage $[v - (f)]$ in the frequency domain, as expressed in

$$V_{\mathrm{TDR}} = V^+(t) + V^-(t) \tag{3}$$

$$\Gamma_M^{2x} = \frac{v^-(f)}{v^+(f)}. \tag{4}$$

Since the 2x-thru has the 1x-fixture and the mirror image of the 1x-fixture, the TDR waveform V_{TDR}^{2x} from the 2x-thru is ideally symmetric by the middle point, and time delay T_{d2x} of the 2x-thru is exactly the same with two times of time delay T_{d1x} from the 1x-fixture. Therefore, TDR waveform V_{TDR}^{1x} of the 1x-fixture can be estimated by the modification of the TDR waveform of the 2x-thru, as shown in Fig. 2(b). The measured reflection ratio Γ_M^{1x} of the 1x-fixture can be expressed in (5), with the actual reflection ratio Γ_A at the middle point. The actual reflection ratio occurs when the characteristic impedance at the middle point is not matched with 50 Ω,

$$\Gamma_M^{1x} = \mathrm{S}_{11}^{1x} + \frac{\left(\mathrm{S}_{21}^{1x}\right)^2}{\frac{1}{\Gamma_A} - \mathrm{S}_{22}^{1x}}. \tag{5}$$

If the impedance at the middle point is 50 Ω, the measured reflection ratio is equal to the return loss1 S_{11}^{1x}. Based on the measured reflection ratio, three unknown variables in the

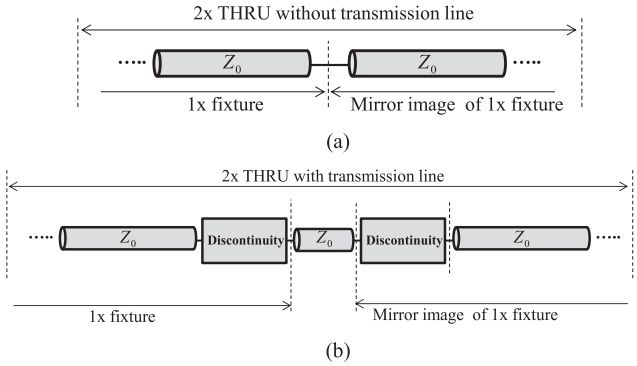

Fig. 3. Design of a 2x-thru without any discontinuity at the end of the 1x-fixture (a) and a 2x-thru with the middle trace between the 1x-fixtures with discontinuity at the end (b).

S-parameters of the 1x-fixture can be calculated as

$$\mathrm{S}_{11}^{1\mathrm{x}} = \frac{\Gamma_A \Gamma_M \mathrm{S}_{11}^{2\mathrm{x}} + \Gamma_A \left(\mathrm{S}_{21}^{2\mathrm{x}}\right)^2 - \Gamma_A \left(\mathrm{S}_{11}^{2\mathrm{x}}\right)^2 - \Gamma_M \mathrm{S}_{21}^{2\mathrm{x}}}{\Gamma_A \Gamma_M - \Gamma_A \mathrm{S}_{11}^{2\mathrm{x}} - \mathrm{S}_{21}^{2\mathrm{x}}} \quad (6)$$

$$\mathrm{S}_{22}^{1\mathrm{x}} = -\frac{\Gamma_A \mathrm{S}_{21}^{2\mathrm{x}} + \mathrm{S}_{11}^{2\mathrm{x}} - \Gamma_M}{\Gamma_A \Gamma_M - \Gamma_A \mathrm{S}_{11}^{2\mathrm{x}} - \mathrm{S}_{21}^{2\mathrm{x}}} \quad (7)$$

$$\mathrm{S}_{21}^{1x} = \frac{\sqrt{\mathrm{S}_{21}^{2x}\left(\Gamma_A^2 - 1\right)\left(\mathrm{S}_{21}^{2x} - \left(\Gamma_M - \mathrm{S}_{11}^{2x}\right)\right)\left(\mathrm{S}_{21}^{2x} + \left(\Gamma_M - \mathrm{S}_{11}^{2x}\right)\right)}}{\Gamma_M \Gamma_A - \Gamma_A \mathrm{S}_{11}^{2x} - \mathrm{S}_{21}^{2x}}. \quad (8)$$

III. Design Criteria and Design Procedure

A. Design Criteria: Discontinuity

If one end of the 1x-fixture is just the transmission line without any discontinuities, the 2x-thru is always easily composed of the 1x-fixture and the mirror image of the 1x-fixture, as shown Fig. 3(a). However, since the 1x-fixture is usually characterized by a discontinuity element such as ball-pad, via, or ground cut, the TCC algorithm will not work if the 2x-thru directly consists of the 1x-fixture and the mirror image of the 1x-fixture, as shown in Fig. 3(a), and eventually a huge error would occur in the calculated S-parameters of the 1x-fixture. In order to calculate the return loss1 $\mathrm{S}_{11}^{1\mathrm{x}}$ of the 1x-fixture correctly, a very short transmission line is necessary between the 1x-fixture and the mirror image of the 1x-fixture, as shown in Fig. 3(b). This additional middle trace should not only be as short as possible, but should also long enough for the TCC algorithm.

The optimized length in the middle trace can be analyzed with two reflected waveforms occurring at discontinuities at the ends of the middle trace, as shown in Fig. 4. If the initial waveform V_{in} with its amplitude V_0 and rise time t_r, as expressed in (9), is injected into the 2x-thru, there is no reflection before an incident waveform meets the first discontinuity

$$v_{\mathrm{in}}(t) = v_0\left(1 - e^{-t/\tau}\right) \quad \tau = t_r/2.197. \quad (9)$$

The first reflection occurs at the first discontinuity between characteristic impedance Z_0 and first input impedance Z_{in1}.

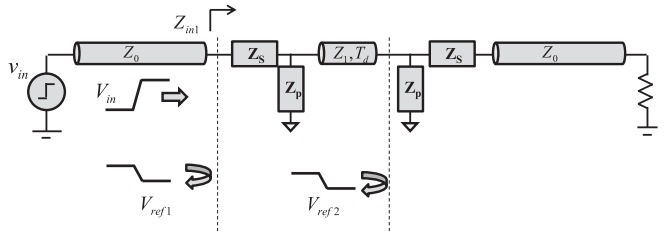

Fig. 4. Two reflected waveforms coming from both discontinuities at the end of the middle trace based on the reflection coefficient.

The first input impedance expressed in (10) comes from the impedances Z_S and Z_P of series and parallel lumped models, due to the discontinuity and the characteristic impedance Z_1 in the middle trace. The reflection coefficient Γ, as expressed in (11), determines the first reflected waveform V_{ref1} in time domain, as expressed as

$$Z_{\mathrm{in1}} = Z_S + Z_P // Z_1 \quad (10)$$

$$\Gamma = \frac{Z_{\mathrm{in1}} - Z_0}{Z_{\mathrm{in1}} + Z_0} \quad (11)$$

$$V_{\mathrm{ref1}}(t) = -\frac{v_0}{2}\left(\exp\left(-\frac{t}{\tau}\right) - 1\right) \frac{Z_1 Z_p - Z_0 Z_1 - Z_0 Z_s + Z_1 Z_s + Z_p Z_s}{Z_0 Z_1 + Z_1 Z_p + Z_0 Z_s + Z_1 Z_s + Z_p Z_s}. \quad (12)$$

The transmitted waveform after the first discontinuity also meets the second discontinuity between the middle trace and the mirror image of the 1x-fixture. The second reflected waveform V_{ref2} arrives at the source after a round-trip time, that is, two times time delay T_d caused by the middle trace. This middle trace gives a short-time delay on TDR-waveform to wait for the first reflected waveform to be stable, before the second reflected waveform V_{r2} arrives.

A new concept of timescale T_{scale} for the design of the 2x-thru is introduced. The voltage fluctuation caused by the first reflected waveform on the TDR waveform is going to be stable after a certain time. This certain time is defined as timescale T_{scale}. If the voltage fluctuation is stable and the second reflected waveform had not arrived yet, the TDR waveform shows the correct impedance in the middle trace on the TDR waveform of the 2x-thru. If not, the calculated return loss1 $S_{11}^{1\mathrm{x}}$ of the 1x-fixture from the modified TDR waveform in (4) has an error due to the misunderstanding of the impedance level at the middle point. Therefore, time delay of the middle trace satisfies the criteria, as expressed

$$T_{\mathrm{scale}} < 2T_d. \quad (13)$$

Based on this criteria in (13), the optimized length of the middle trace to remove the error in return loss1 $\mathrm{S}_{11}^{1\mathrm{x}}$ of the 1x-fixture can be estimated, as expressed in (14). The length of the middle trace is basically affected by not only the timescale, but also the effective dielectric constant e_{eff} and the velocity of light V_c,

$$\mathrm{Length} > \frac{v_c T_{\mathrm{scale}}}{2\sqrt{e_{\mathrm{eff}}}}. \quad (14)$$

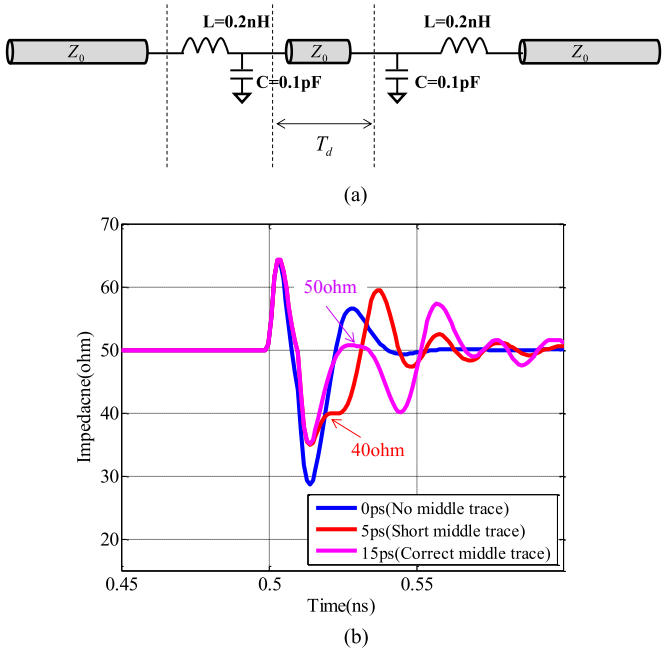

Fig. 5. 2x-thrus with a discontinuity between 1x-fixtures and the middle trace (a) three different TDR waveforms depending on different time delays caused by the middle trace (b).

A 1x-fixture with discontinuities, consisting of a lumped inductor and capacitor at the end, was investigated to see the effect of timescale from the middle trace. Both the inductor and capacitor have values 0.2 nH and 0.1 pF, respectively. The structure of the 2x-thru for TCC is shown in Fig. 5(a). The input impedance at the first discontinuity along with the 2x-thru in the frequency domain is expressed in (15). For convenient analysis, the characteristic impedance of the middle trace is the same as that of the 1x-fixture

$$Z_{\text{in}}(\omega) = j\omega L + \left(\frac{1}{j\omega C}\right) // Z_0. \tag{15}$$

The unit step pulse v_{in} has 10 ps of 10–90% rise time $[t_r]$ and 1 V of amplitude v_0, as expressed in (9). The first reflected waveform only caused by the first discontinuity has 24.3 ps of calculated timescale to make a stable reflection. Therefore, two times longer time delay T_d, obtained from the middle trace is necessary. To validate this condition effect on the TDR waveform, three different middle traces with different time delays of 0, 5, and 15 ps, respectively, were inserted between the 1x-fixture and the mirror image of 1x-fixture. Fig. 5(b) shows three different TDR waveforms of the 2x-thru, depending on different lengths in the middle trace. The blue curve is the TDR waveform of the 2x-thru without the middle trace. Thus, it is impossible to build the TDR waveform for the 1x-fixture. On the red TDR waveform, the impedance at the middle point is not 50 Ω rather it is 40 Ω, if the middle trace is not long enough to see the impedance at the middle point. The pink TDR waveform clearly shows that the second reflected waveform arrives before the timescale, since the 15 ps time delay in the middle trace satisfies the design criteria in (14).

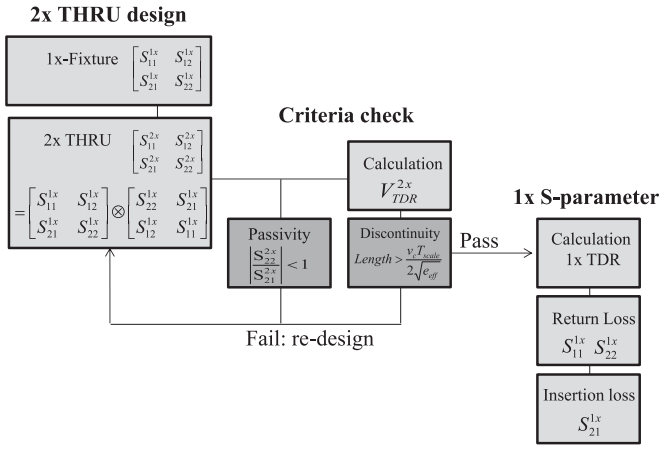

Fig. 6. Design procedure with two design criteria for the 2x-thru design for the error reduction in S-parameters.

B. Design Criteria 2: Passivity

Another design criteria for the 2x-thru is passivity. The magnitude of the calculated return loss2 S_{22}^{1x} should be always less than 1, as expressed in (16). If not, calculated S-parameters of the 1x-fixture violates the passivity

$$\left|S_{22}^{1x}\right| = \left|\frac{S_{22}^{2x}}{S_{21}^{2x}} - \frac{S_{11}^{1x}}{S_{21}^{2x}}\right| \le 1 \tag{16}$$

$$\left|S_{22}^{1x}\right| = \left|\frac{S_{22}^{2x}}{S_{21}^{2x}} - \frac{S_{11}^{1x}}{S_{21}^{2x}}\right| \le \left|\frac{S_{22}^{2x}}{S_{21}^{2x}}\right| + \left|-\frac{S_{11}^{1x}}{S_{21}^{2x}}\right| \tag{17}$$

$$\left|\frac{S_{22}^{2x}}{S_{21}^{2x}}\right| < 1. \tag{18}$$

$|S_{22}^{1x}|$ is always less than or equal to a summation of two magnitudes, as expressed in (17). Whereas the second term $|-S_{11}^{1x}/S_{21}^{2x}|$ is unknown before applying TCC; only $|S_{22}^{2x}/S_{21}^{2x}|$ can be calculated before applying TCC based on the S-parameters of the 2x-thru. In order to get rid of a very small possibility for a passivity fail, at least $|S_{22}^{2x}/S_{21}^{2x}|$ is always less than 1, as expressed in (18), the second criteria for the design of the 2x-thru. If $|S_{22}^{2x}/S_{21}^{2x}|$ is larger than 1, calculated $|S_{22}^{1x}|$ is always greater than 1, whatever $|-S_{11}^{1x}/S_{21}^{2x}|$ is.

C. Design Procedure

In order to apply the TCC algorithm to the symmetric 2x-thru and get reliable S-parameters of the asymmetric 1x-fixture, an appropriate design procedure shown in Fig. 6 is necessary. First of all, 2x-thru should be designed based on the 1x-fixture and the mirror image of the 1x-fixture. Both the 1x-fixture and the 2x-thru should not only be passive, but also reciprocal. Then, it is necessary for the 2x-thru to check the two design criteria regarding discontinuity and passivity based on the calculated TDR waveform and S-parameters from the 2x-thru. If one of the two criteria fail, the 2x-thru should be redesigned till both criteria are satisfied. If the designed 2x-thru satisfies the two criteria, the modified TDR waveform for the 1x-fixture is correctly obtained to see the impedance at the middle point. The actual

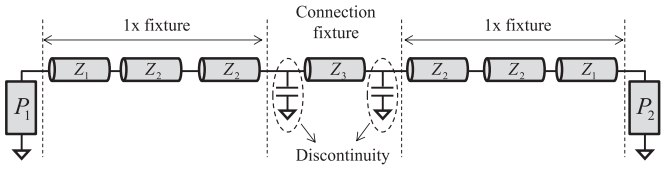

Fig. 7. Three 2x-thrus consisting of ideal lumped elements to see the error amplification in S-parameters of the 1x-fixture when design criteria fails.

reflection ratio Γ_A at the middle point is calculated with the characteristic impedance at the middle point and 50 Ω. Return loss1 S_{11}^{1x} can be obtained based on the modified TDR wave for the 1x-fixture. After that, the rest, return loss2 S_{22}^{1x} and IL S_{21}^{1x} of the 1x-fixture, are calculated in order.

D. Error Sensitivity

While return loss1 S_{11}^{1x} is obtained from the modified TDR waveform of the 1x-fixture, IL S_{21}^{1x} and return loss2 S_{22}^{1x} in the S-parameters of the 2x-thru, can be calculated with return loss1 S_{11}^{1x}. Therefore, the other two terms would generate an error if the calculated return loss1 S_{11}^{1x} has an error itself. Since there is no way to know the original S-parameters of the 1x-fixture for comparison with the calculated S-parameters through TCC in the real workplace, it is important to analyze how a small error in return loss1 S_{11}^{1x} can eventually affect the other two terms, IL S_{21}^{1x} and return loss2 S_{22}^{1x}. This is called the error sensitivity in TCC to check S-parameter reliability of the 1x-fixture, analyzed in advance with known S-parameters of the 2x thru. The sensitivity for return loss2 S_{22}^{1x} is expressed in (19). The term "*d*" in (19) stands for the difference, and it means a small error between the original and calculated S-parameters

$$d\left|S_{22}^{1x}\right| = \frac{1}{\left|S_{21}^{2x}\right|} d\left|S_{11}^{1x}\right|. \tag{19}$$

The return loss error coefficient (RLEC) represents how much the error in return loss1 S_{11}^{1x} is amplified at return loss2 S_{22}^{1x}, defined as $1/|S_{21}^{2x}|$, as expressed in (20). As the 2x-thru has a higher IL, the error in return loss2 S_{22}^{1x} is much larger

$$\text{RLEC} = \frac{d\left|S_{22}^{1x}\right|}{d\left|S_{11}^{1x}\right|} = \frac{1}{\left|S_{21}^{2x}\right|}. \tag{20}$$

On the other hand, the sensitivity of IL S_{21}^{1x} is more complicated, as expressed in (21). Hence, the insertion loss error coefficient (ILEC) is defined as expressed in (22):

$$d\left|S_{21}^{1x}\right| = \frac{\left|S_{11}^{2x} - S_{11}^{1x}\right|}{\left|S_{21}^{1x}\right|\left|S_{21}^{2x}\right|} d\left|S_{11}^{1x}\right| \tag{21}$$

$$\text{ILEC} = \frac{d\left|S_{21}^{1x}\right|}{d\left|S_{11}^{1x}\right|} = \frac{\left|S_{11}^{2x} - S_{11}^{1x}\right|}{\left|S_{21}^{1x}\right|\left|S_{21}^{2x}\right|}. \tag{22}$$

If the channel is too lossy, two return losses from the 1x-fixture and the 2x thru are close to each other and its subtraction value approaches 0. Therefore, even though a reciprocal of the multiplication of two insertion losses in (22) has a large number; ILEC is very close to 0, if the channel is lossy. It means that the small error in return loss1 S_{11}^{1x} is not dominantly amplified in insertion loss S_{21}^{1x} of the 1x-fixture.

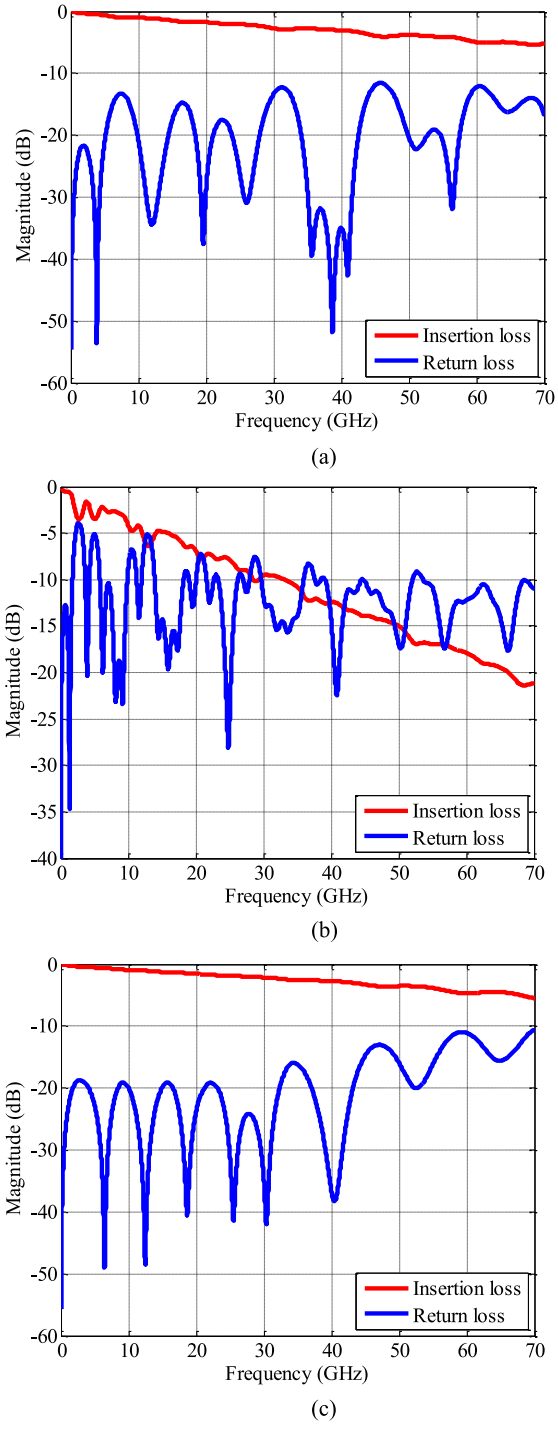

Fig. 8. Fixture A is a standard 2x-thru without criteria violations to bring errors in S-parameters of the 1x-fixture (a). Fixture B violates passivity criteria due to large IL, then $|S_{22}^{2x}/S_{21}^{2x}|$ is greater than 1 at high frequency (b). Fixture C violates discontinuity criteria due to a short middle trace between the 1x-fixture (c).

IV. Verification With Text Fixtures

The design of the 2x-thru in the TCC procedure reduces the error between S-parameters. In other words, if the 2x-thru violates one of the two design criteria in the TCC procedure, calculated S-parameters of the 1x-fixture through TCC has a huge

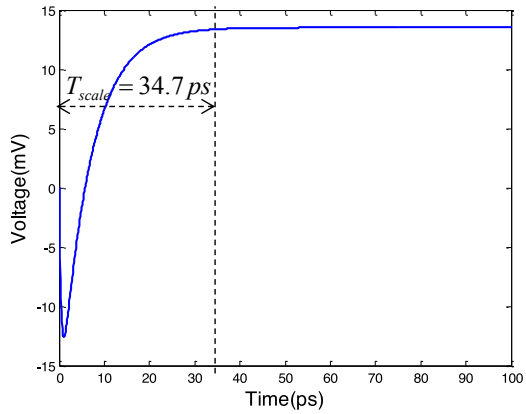

Fig. 9. Reflected waveform occurring at the first discontinuity behaves as a capacitor as expected and 34.7 ps of timescale $T_{\rm scale}$ is necessary to see the characteristic impedance.

error. However, since the reference S-parameters do not exist in real channel characterization, there is no way to know how criteria violation affects final S-parameters of the 1x-fixture. Thus, three different 2x-thrus consisting of ideal lumped elements, as shown in Fig. 7, were investigated to see the effect of error amplification depending on violations in design criteria. This way provides the reference S-parameters of the 1x-fixture to compare with S-parameters through TCC.

While Fixture A is a standard 2x-thru with a low IL less than the RL within all frequency ranges and optimized length of the middle trace between 1x-fixtures, both Fixture B and Fixture C violate either of the two design criteria in the TCC procedure, as shown in Fig. 8. Fixture B has a large IL at high frequency, so the passivity violates design criteria due to $|S_{22}^{2x}/S_{21}^{2x}|$ being greater than 1. Thus, S-parameters of the 1x-fixture at high frequency would become nonpassive, or have larger error amplification. On the other hand, Fixture C has a similar low IL, but shorter middle trace to fail the discontinuity criteria. In order to calculate the minimum length of the middle trace based on timescale $T_{\rm scale}$ in (14), the first reflected waveform from the first discontinuity is shown in Fig. 9. The discontinuity behaves as a capacitor, and its dip is much lower than the characteristic impedance along a line and needs 34.7 ps of timescale $T_{\rm scale}$ to come back to the characteristic impedance.

Based on calculated timescale $T_{\rm scale}$, the minimum length of the middle trace should be longer than 2.86 mm, as expressed in (14). Since Fixture A, Fixture B, and Fixture C have 5, 5, and 1 mm as a length in the middle trace, respectively. While both Fixture A and Fixture B satisfy the discontinuity criteria, Fixture C has a much shorter length than the minimum length and, thus, violates the discontinuity criteria. The calculated return loss1 S_{11}^{1x} for Fixture A and Fixture B, based on the modified TDR waveform for the 1x-fixture, are the same as a simulated RL obtained from an ideal 1x-fixture, as shown in Fig. 10. However, calculated return loss1 S_{11}^{1x} for Fixture C shows a totally different tendency compared to reference return loss1 S_{11}^{1x}. Therefore, the other two terms, IL S_{21}^{1x} and return loss2 S_{22}^{1x}, cannot be calculated correctly. Return loss1 S_{11}^{1x} in Fig. 10 shows that the calculated return loss1 S_{11}^{1x} of the 1x-fixture through

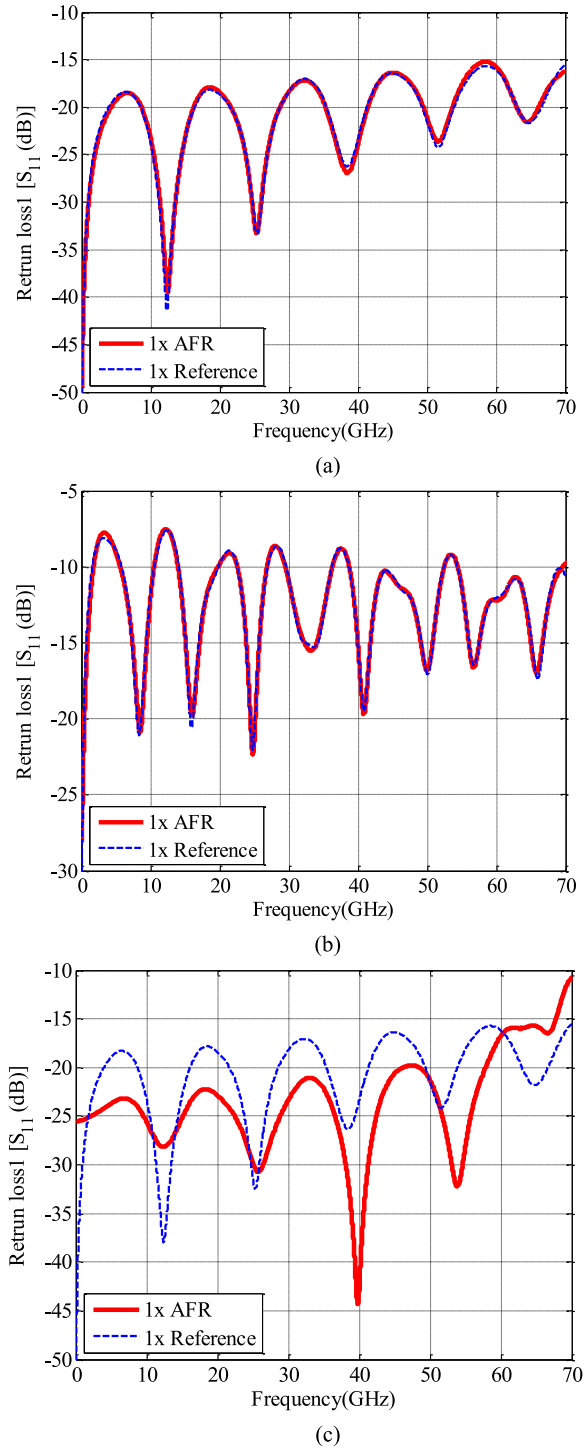

Fig. 10. Comparison of calculated return loss1 S_{11}^{1x} based on the modified TDR waveform for a 1x-fixture and simulated return loss1 S_{11}^{1x} obtained from the ideal 1x-fixture in case of Fixture A (a), Fixture B (b), and Fixture C (c), respectively.

TCC is not correct, if the middle trace has a shorter length than the optimized one.

In order to check the passivity criteria in the TCC procedure, $|S_{22}^{2x}/S_{21}^{2x}|$ of the 2x-thru should be investigated. If $|S_{22}^{2x}|/|S_{21}^{2x}|$ is less than 1, at least, the magnitude of calculated return loss2 $|S_{22}^{1x}|$ can be less than 1, which means that there is no passivity

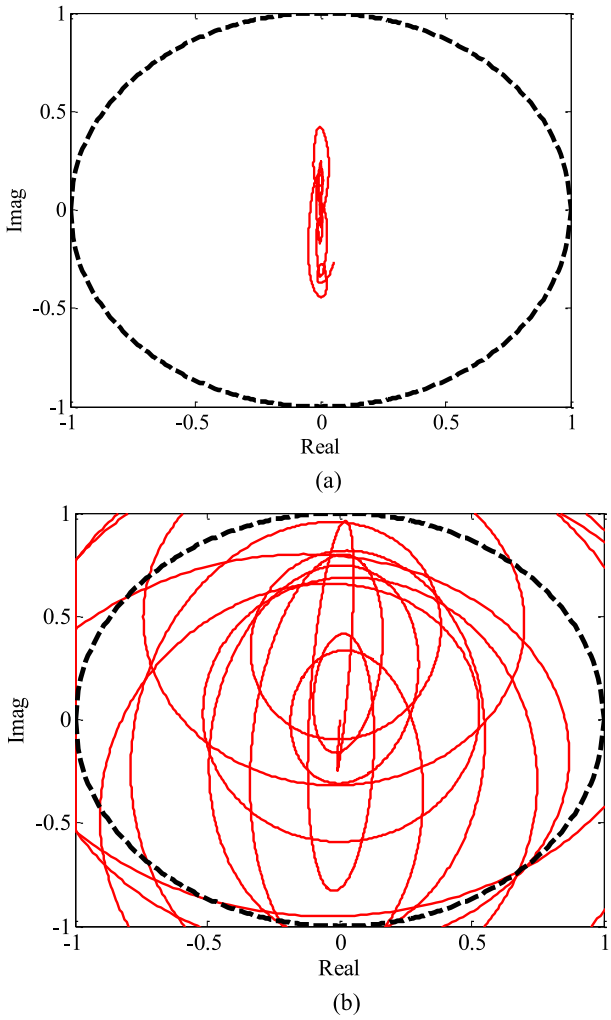

Fig. 11. Complex plane with a unit circle to check the passivity criteria in the TCC procedure. $|S_{22}^{2x}/S_{21}^{2x}|$ in Fixture A (a) and $|S_{22}^{2x}/S_{21}^{2x}|$ in Fixture B (b) are plotted respectively on the complex plane.

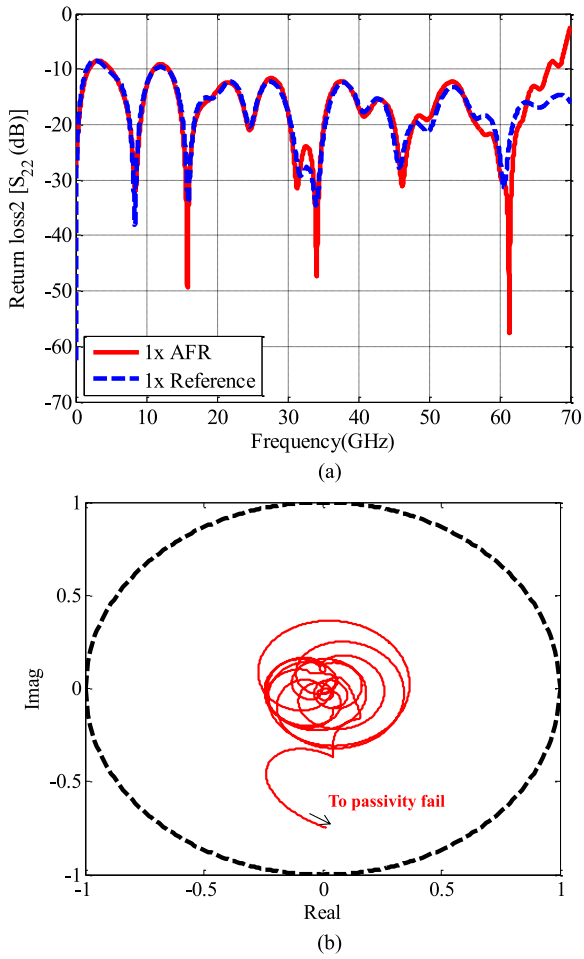

Fig. 12. Calculated return loss2 S_{22}^{1x} in Fixture B has a small error between 30 and 60 GHz and goes to 0 dB after 60 GHz (a). Return loss2 S_{22}^{1x} after 60 GHz on the complex plane is approaching the unit circle (b).

violation in the calculated S-parameters of the 1x-fixture through TCC. The complex plane is appropriate to check the passivity criteria, as shown in Fig. 11. Since Fixture C already violates the discontinuity criteria, only Fixture A and Fixture B were investigated. The black dot line is a unit circle to determine whether the 2x-thru violates the passivity criteria or not, and the red solid line shows the calculated $|S_{22}^{2x}/S_{21}^{2x}|$ obtained from S-parameters of the 2x-thru. While $|S_{22}^{2x}/S_{21}^{2x}|$ from Fixture A always exists inside the unit circle, $|S_{22}^{2x}/S_{21}^{2x}|$ from Fixture B sometimes crosses the unit circle. Therefore, return loss2 S_{22}^{1x} in S-parameters of Fixture B through TCC is not always nonpassive, but sometimes nonpassive.

Since $|S_{22}^{2x}/S_{21}^{2x}|$ in Fixture B sometimes fails to be inside the unit circle, the calculated return loss2 S_{22}^{1x} has a huge error amplification at high frequency, and then approaches the nonpassive line "0" as shown in Fig. 12(a). In the complex plane, as the frequency goes higher, the calculated return loss2 S_{22}^{1x} approaches the unit circle which determines the passivity violation, as shown in Fig. 12(b).

Finally, Fixture A is only 2x-thru to correctly calculate S-parameters through TCC, as shown in Fig. 13. While IL S_{21}^{1x} from TCC and ideal simulation agrees well, return loss2 S_{22}^{1x} agrees only up to 64 GHz. This error comes from a small error in magnitude and phase, at the same time between calculated return loss1 S_{11}^{1x} and simulated return loss1 S_{11}^{1x}. As seen in Fig. 13, error deviation in return loss2 S_{22}^{1x} is much larger, and starts at a lower frequency than the IL.

Though calculated return loss1 S_{11}^{1x} looks perfectly matched with the simulated return loss1, there is still a very small error between them, as shown in Fig. 14. While the maximum error is -2.66 dB occurring at 12.2 GHz, the maximum error return loss2 S_{22}^{1x} occurs at the end of the frequency range. As explained in error sensitivity in TCC, there are two error coefficients, RLEC and ILEC, to amplify the small error in return loss1 S_{11}^{1x}. Based on S-parameters of Fixture A, two error coefficients are calculated, as shown in Fig. 15. While RLEC linearly increases as frequency increases, ILEC stays at a low level within the entire frequency range. Since RLEC is always higher than 1, the dominant error amplification caused by the small error occurs at return loss2 S_{22}^{1x} than IL S_{21}^{1x}. As long as the fixture is passive,

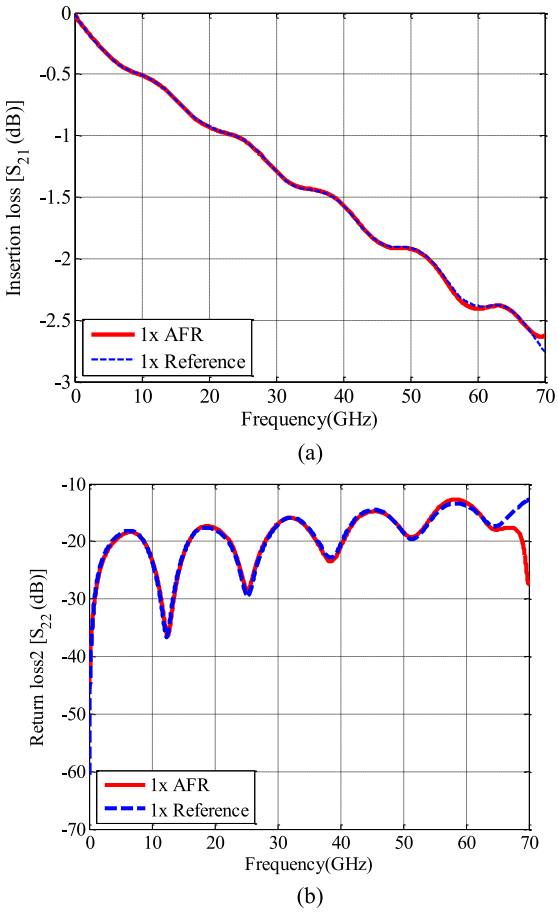

Fig. 13. Calculated IL S_{21}^{1x} (a) and return loss2 S_{22}^{1x} (b) of Fixture A through TCC. Both IL and RL agrees up to almost 64 GHz.

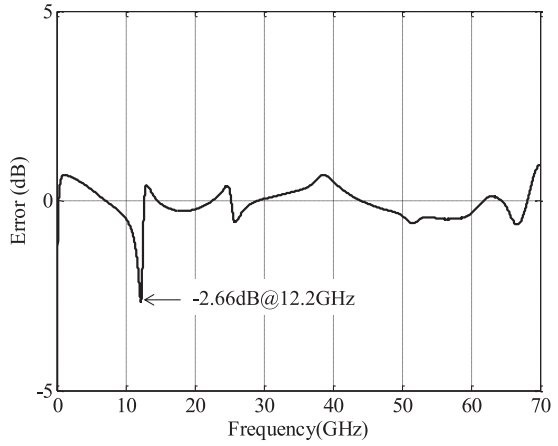

Fig. 14. Small error between calculated return loss1 obtained from TCC and simulated return loss1 coming from ideal 1x-fixture in ADS. The maximum error is −2.66 dB at 12.2 GHz.

ILEC is always less than 1, and it never amplifies the small error in IL.

Based on the small error in return loss1 S_{11}^{1x}, error deviation in IL S_{21}^{1x} and return loss2 S_{22}^{1x} shows different tendency as the frequency goes up, as shown in Fig. 16. The error in return loss2

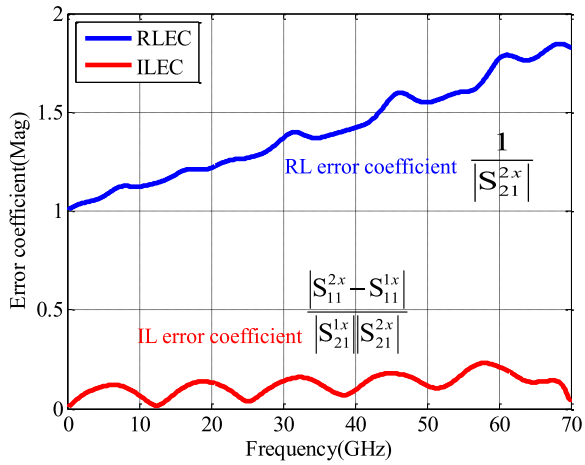

Fig. 15. Two error coefficients for return loss2 S_{22}^{1x} and IL S_{21}^{1x}. While RLEC linearly increases as frequency goes higher, ILEC has periodic value and its value is very low. As long as the fixture is passive, ILEC is always less than 1 and it never amplifies small error in IL S_{21}^{1x}.

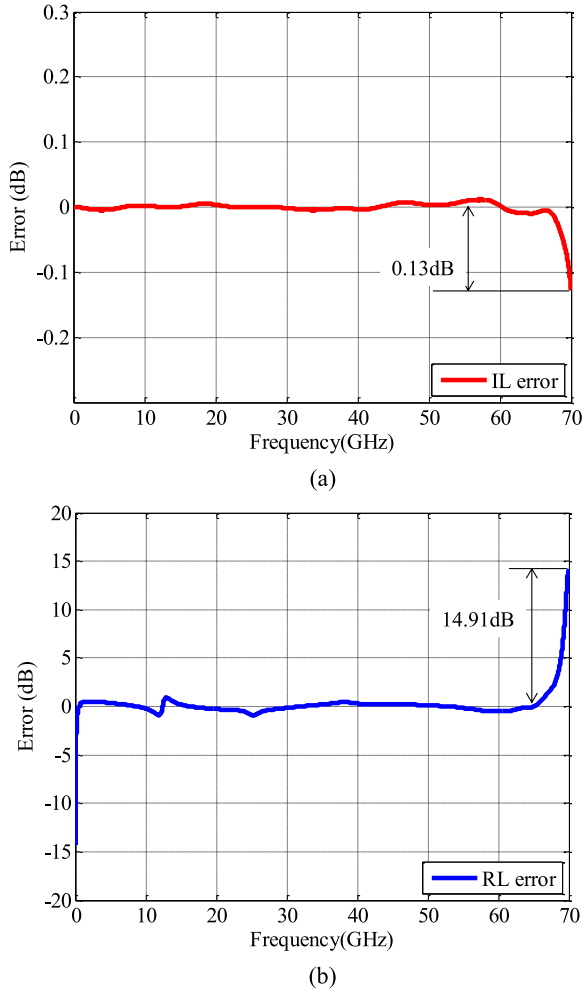

Fig. 16. Error deviation in IL S_{21}^{1x} (a) and return loss2 S_{22}^{1x} (b). Since RLEC is much larger than 1 in general, return loss2 S_{22}^{1x} is much more sensitive than IL in error amplification.

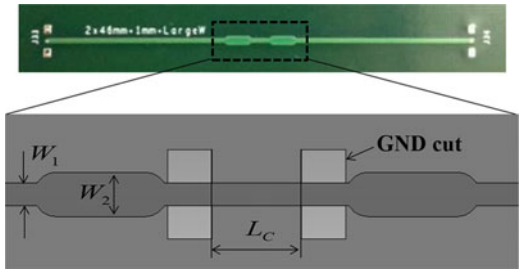

Fig. 17. TCC fixture on PCB with artificial discontinuities and 1000 um GSG probes at both ends. Different lengths are designed between two fixtures.

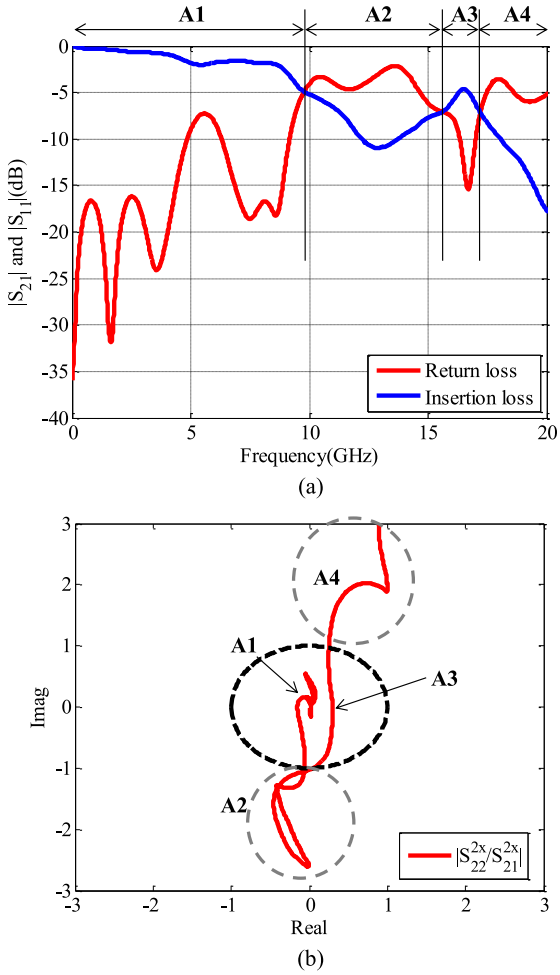

Fig. 18. IL and RL in S-parameters of the 2*x*-thru to check passivity criteria in the TCC procedure (a). $|S^{2x}_{22}/S^{2x}_{21}|$ on real and image plot with unit circle shown as black dot circle (b).

S^{1x}_{22} is much larger than the original small error in return loss1 S^{1x}_{11}, because RLEC is larger than 1. In general TCC, a small error in return loss1 S^{1x}_{11} is greatly amplified at return loss2 S^{1x}_{22}.

V. Experimental Verification

TCC fixtures for the experimental verification were fabricated on PCB, as shown in Fig. 17. Artificial discontinuities, such as wider width W_2 and GND cut, were designed at the end of the 1x-fixture. The middle trace between 1x-fixtures has 3, 4, 5, and 6 mm of different lengths L_c. GSG 1000 μm pads at both ends were designed.

In order to check the passivity criteria for the 2x-thru, measured IL and RL are put together, as shown in Fig. 18(a).

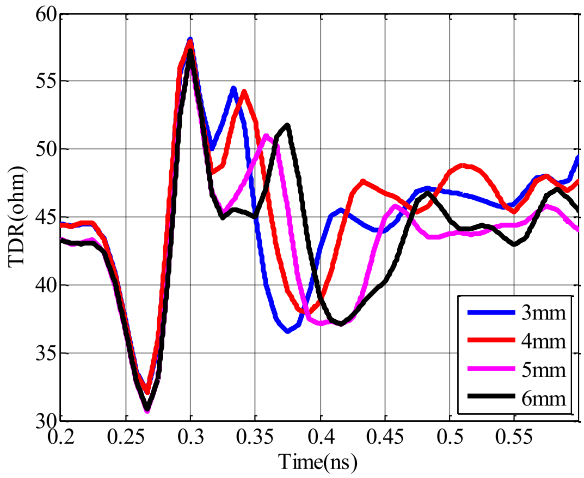

Fig. 19. TDR waveforms in differing lengths of the middle trace. 5 and 6 mm clearly show the impedance at the middle point and satisfy discontinuity criteria in TCC procedure.

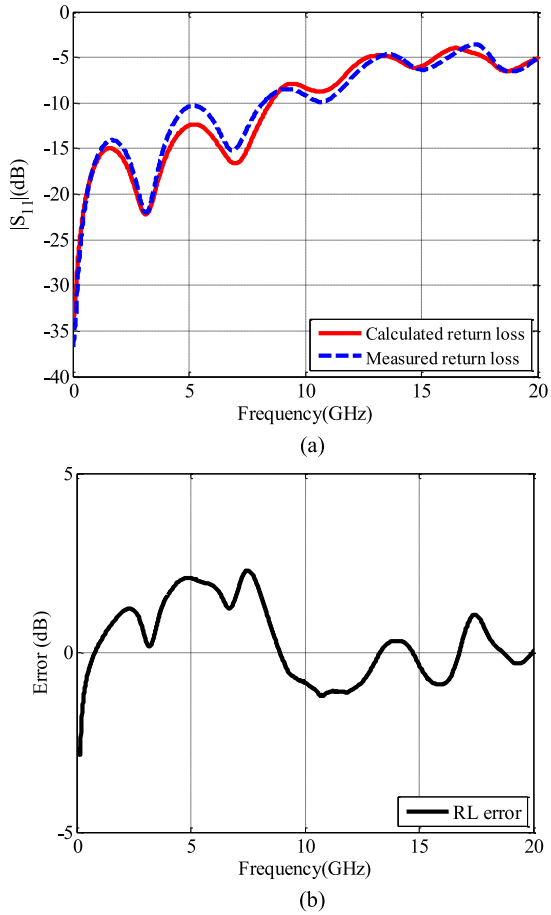

Fig. 20. Calculated return loss1 S^{1x}_{11} based on modified TDR waveform (a) and the difference between the measurement and the calculation (b).

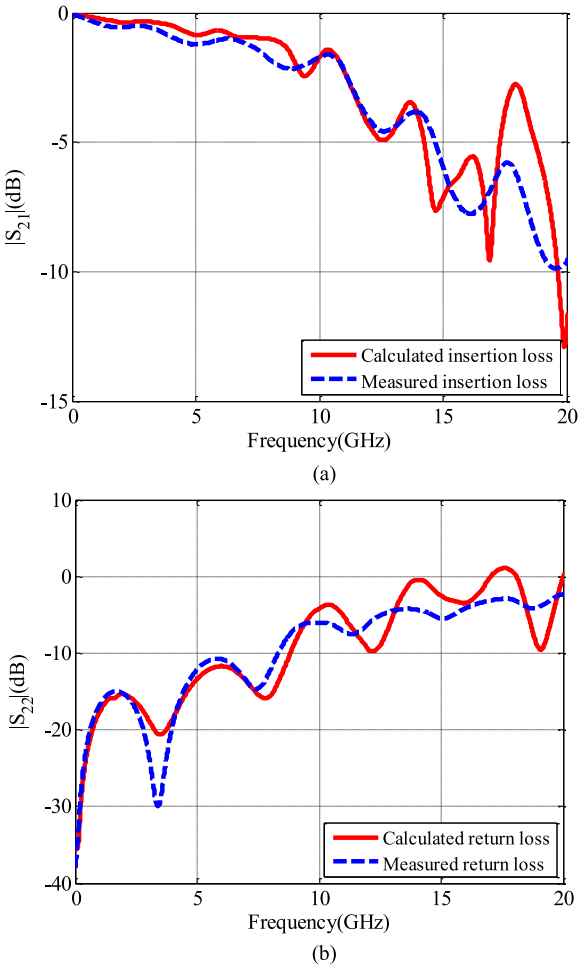

Fig. 21. Calculated and measured IL S_{21}^{1x} (a) and return loss2 S_{22}^{1x} (b) based on calculated return loss 1 S_{11}^{1x}.

Although both Area 1 A1 and Area 3 A3 satisfy the passivity criteria inside the unit circle, shown as a black dot circle, Area 2 A2 and Area 4 A4 are out of the unit circle. Therefore, S-parameters through TCC has high reliability only up to around 10 GHz, and the small error in return loss1 S_{11}^{1x} will be amplified in IL S_{21}^{1x} and return loss2 S_{22}^{1x}. The discontinuity criteria in the TCC procedure is checked with the TDR waveform, as shown in Fig. 19. The trace impedance at the middle point is around 45 Ω. Although at short lengths of the middle trace, such as 3 and 4 mm, the impedance at the middle point is harder to see; the length longer than 5 mm clearly represents the impedance at the middle point. Therefore, return loss1 S_{11}^{1x} from TCC for the 1x-fixture is calculated correctly without an error amplification.

The return loss1 S_{11}^{1x} of the 1x-fixture based on the modified TDR waveform is obtained, as shown in Fig. 20(a). Both the measured RL and calculated RL agreed up to 20 GHz with a maximum 2-dB error, as shown in Fig. 20(b).

Therefore, IL S_{21}^{1x} and return loss2 S_{22}^{1x} of the 1x-fixture are calculated based on obtained return loss1 S_{11}^{1x}, as shown in Fig. 21. Although both IL S_{21}^{1x} and RL S_{22}^{1x} agreed with a small error within 10 GHz, a huge oscillation occurs after around 10 GHz. The error between measurement and calculation at frequency lower than 10 GHz mostly comes from the small error in return loss1 S_{11}^{1x}, as shown in Fig. 20(b). However, the large error at frequency higher than 10 GHz is caused by not only the existing error in return loss1 S_{11}^{1x}, but also the error amplification due to the failure of the passivity criteria. In TCC, there are two areas, the one for the reliable zone, where the 2x-thru satisfies the passivity criteria, and the other for the distrusted zone, as shown in Fig. 18. As a result, the failure of the passivity check results in a huge error amplification after around 10 GHz in IL S_{21}^{1x} and return loss2 S_{22}^{1x} through TCC.

VI. Conclusion

A TCC algorithm for asymmetric fixture characterization was introduced. Analytical two design criteria of discontinuity and passivity, and a procedure to reduce the errors in TCC were proposed. Moreover, error sensitivity through TCC was analyzed to estimate error amplification with ILEC and RLEC. The proposed design criteria and analysis in terms of TCC were validated with a fabricated 2x-thru and 1x-fixture on a PCB through the experimental measurement.

References

[1] J. Zhang, Q. B. Chen, K. Qiu, A. C. Scogna, M. Schauer, G. Romo, J. L. Drewniak, and A. Orlandi, "Design and modeling for chip-to-chip communication at 20 Gbps," in *Proc. IEEE Int. Symp. Electromagn. Compat.*, Fort Lauderdale, FL, USA, 2010, pp. 467–472.

[2] Q. B. Chen, J. Zhang, K. Qiu, D. Padilla, Z. Yang, A. C. Scogna, and J. Fan, "Enabling terabit per second switch linecard design through chip/package/PCB co-design," in *Proc. IEEE Int. Symp. Electromagn. Compat.*, Fort Lauderdale, FL, USA, 2010, pp. 585–590.

[3] W. T. Beyene, X. Yuanz, N. Cheng, and H. Shi, "Design, modeling, and hardware correlation of a 3.2 Gbps pair memory channel," *IEEE Adv. Packag.*, vol. 27, no. 1, pp. 34–44, Feb. 2004.

[4] M. Hiebel, "Measurement Accuracy and Calibration," in *Fundamental Vector Network Analysis*, 5th ed. Germany: Rohde & Schwarz, 2011, pp. 109–131.

[5] J. Zhang, Q. B. Chen, Z. Qiu, J. L. Drewniak, and A. Orlandi, "Using a single-ended TRL calibration pattern to de-embed coupled transmission lines," in *Proc. IEEE Int. Symp. Electromagn. Compat.*, Austin, TX, USA, 2009, pp. 197–202.

[6] J. Dunsmore, N. Cheng, and Y.-X. Zhang, "Characterizations of asymmetric fixtures with a two-gate approach," in *Proc. Microw. Meas. Conf.*, Baltimore, MD, USA, 2011, pp. 1–6.

[7] H. Barnes, "Advances in ATE fixture performance and socket characterization for multi-gigabit applications," presented at the DesignCon, San Jose, CA, USA, 2012.

[8] V. Adamian and B. Cole, "A novel procedure for characterization of multiport high speed balanced devices," presented at the DesignCon, San Jose, CA, USA, 2007.

Changwook Yoon (S'05–M'12) received the B.S., M.S., and Ph.D. degree in electrical engineering from the Korea Advanced Institute of Science and Technology, Daejeon, Korea, in 2005, 2007, and 2010, respectively.

He was an Assistant Visiting Research Professor with the Missouri University of Science and Technology, Rolla, MO, USA, for two years, and a Senior Engineer with the Samsung Advanced Institute of Technology, Giheung, Korea, for two years. He is currently a Member of Technical Staff at Altera, San Jose, CA, USA, and working on signal/power integrity analysis of various parallel interfaces. He has a total of nine years of research experience with signal/power integrity on silicon, package, and PCB.

Mikheil Tsiklauri (M'12) received the B.S., M.S., and Ph.D. degrees in applied mathematics from Tbilisi State University, Tbilisi, Georgia, in 1998, 2000, and 2003, respectively.

From 2000 to 2012, he was with Tbilisi State University. He is currently a Research Professor with the Missouri University of Science and Technology, Rolla, MO, USA. His research interests include applied mathematics and algorithms.

Mikhail Zvonkin received the B.S. and M.S. degrees in mathematics from Lomonosov Moscow State University, Moscow, Russia, in 2012. He is currently working toward the M.S. degree in electrical engineering with the EMC Laboratory of Missouri University of Science and Technology, Rolla, MO, USA.

His main research interests include mathematical modeling for high-speed link path analysis, methods for checking and enforcing causality, numerical methods, and scientific computing.

Qinghua Bill Chen received the B.S.E.E. and M.S.E.E. degrees from Tsinghua University, Beijing, China, and the Ph.D. degree from Texas A&M University, College Station, TX, USA.

From 2002 to 2010, he was with Cisco systems, Inc., San Jose, CA, USA, through Andiamo Systems, Inc., acquisition, as a Senior Manager and a Technical Leader, where he was In-Charge of high-performance data center product research and development. Prior to this, he was also with Raza Foundries, Inc., Nplab, Inc., and Texas Instruments, Inc., as a Technical Leader/ Senior Design Engineer, where he was engaged in high-speed IC/system designs.He is currently a Professor and the Head of the Information Technology Department, Yangtze Delta Region Institute of Tsinghua University, Zhejiang, China. His main research interests include high-performance networking system architectures, energy efficient data center design, and high speed system signal integrity and power integrity design methodologies.

Alexander Razmadze received the B.S., M.S., and Ph.D. degrees in physics, with focus on computational electromagnetics, from Tbilisi State University, Tbilisi, Georgia.

He is currently a Senior Product Engineer at Altera Corporation, San Jose, CA, USA. Prior to joining Altera in 2013, he was working with the Missouri University of Science and Technology (formerly known as the University of Missouri-Rolla), Rolla, as Postdoctoral Fellow, since 2010, where his research interests included electromagnetic compatibility of high-speed digital electronics, signal integrity, and numerical electromagnetic analysis. His current research interests include signal integrity in high-speed digital systems, on-chip and system-level power delivery network design and modeling, jitter, and timing impact from on-chip PDN noise, as well as the development of 28 +Gb/s test fixture de-embedding algorithms and techniques.

Aman Aflaki received the M.S.E.E. degree in electrical engineering from the Missouri University of Science and Technology, Rolla, MO, USA.

He is currently the Manager of Transceiver Test Group with Altera Corporation, San Jose, CA, USA, where he is responsible for transceiver DFT, test development, hardware design and signal integrity for next generation FPGAs. He has published papers in IEEE TRANSACTIONS ON INSTRUMENTATION AND MEASUREMENT, ECTC, and DesignCon, and holds two patents in the field of signal integrity for wafer sort testing.

Jingook Kim (M'09) received the B.S., M.S., and Ph.D. degrees in electrical engineering from the Korea Advanced Institute of Science and Technology, Daejon, Korea, in 2000, 2002, and 2006, respectively.

From 2006 to 2008, he was a Senior Engineer with DRAM Design Team in Memory Division of Samsung Electronics, Hwasung, Korea. From January 2009 to July 2011, he was a Postdoctoral Fellow with the EMC Laboratory, Missouri University of Science and Technology, MO, USA. In July 2011, he joined the Ulsan National Institute of Science and Technology, Ulsan, Korea, where he is currently an Assistant Professor. His current research interests include high-speed I/O circuits design, 3D-IC, EMC, ESD, and RF interference.

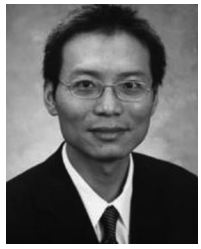

Jun Fan (S'97–M'00–SM'06) received the B.S. and M.S. degrees in electrical engineering from Tsinghua University, Beijing, China, in 1994 and 1997, respectively, and the Ph.D. degree in electrical engineering from the University of Missouri-Rolla, Rolla, MO, USA, in 2000.

From 2000 to 2007, he was a Consultant Engineer with NCR Corporation, San Diego, CA, USA. In July 2007, he joined the Missouri University of Science and Technology (formerly University of Missouri-Rolla), and is currently an Associate Professor with the EMC Laboratory, Missouri S&T, Rolla. His research interests include signal integrity and EMI designs in high-speed digital systems, dc power-bus modeling, intrasystem EMI and RF interference, PCB noise reduction, differential signaling, and cable/connector designs.

Dr. Fan was the Chair of the IEEE EMC Society TC-9 Computational Electromagnetics Committee from 2006 to 2008, and was a Distinguished Lecturer of the IEEE EMC Society in 2007 and 2008. He is currently the Vice Chair of the Technical Advisory Committee of the IEEE EMC Society, and is an Associate Editor for the IEEE TRANSACTIONS ON ELECTROMAGNETIC COMPATIBILITY and EMC Magazine. He received the IEEE EMC Society Technical Achievement Award in August 2009.

James L. Drewniak (F'07) received the B.S. (Highest Hons.), M.S., and Ph.D. degrees in electrical engineering from the University of Illinois at Urbana-Champaign, Champaign, IL, USA.

He is with Electromagnetic Compatibility Laboratory, Missouri University of Science and Technology, MO, USA.